

Extra Dimensions are Dark: II Fermionic Dark Matter

Thomas G. Rizzo [†]

SLAC National Accelerator Laboratory 2575 Sand Hill Rd., Menlo Park, CA, 94025 USA

Abstract

Extra dimensions can be very useful tools when constructing new physics models. Previously, we began investigating toy models for the 5-D analog of the kinetic mixing/vector portal scenario where the interactions of bulk dark matter with the brane-localized fields of the Standard Model are mediated by a massive $U(1)_D$ dark photon also living in the bulk. In that setup, where the dark matter was taken to be a complex scalar, a number of nice features were obtained such as $U(1)_D$ breaking by boundary conditions without the introduction of a dark Higgs field, the absence of potentially troublesome SM Higgs-dark singlet mixing, also by boundary conditions, the natural similarity of the dark matter and dark photon masses and the decoupling of the heavy gauge Kaluza-Klein states from the Standard Model. In the present paper we extend this approach by examining the more complex cases of Dirac and Majorana fermionic dark matter. In particular, we discuss a new mechanism that can occur in 5-D (but not in 4-D) that allows for light Dirac dark matter in the ~ 100 MeV mass range, even though it has an s -wave annihilation into Standard Model fields, by avoiding the strong constraints that arise from both the CMB and 21 cm data. This mechanism makes use of the presence of the Kaluza-Klein excitations of the dark photon to extremize the increase in the annihilation cross section usually obtained via resonant enhancement. In the Majorana dark matter case, we explore the possibility of a direct s -channel dark matter pair-annihilation process producing the observed relic density, due to the general presence of parity-violating dark matter interactions, without employing the usual co-annihilation mechanism which is naturally suppressed in this 5-D setup.

[†]rizzo@slac.stanford.edu

1 Introduction

Although its true nature remains in the realm of speculation, the presence of dark matter (DM) clearly signals the existence of new physics beyond the Standard Model (SM). However, we don't yet know if DM interacts other than gravitationally with the SM. Models that attempt to calculate the observed DM relic density generally postulate that such interactions must exist but they are likely to be far weaker than the known weak interactions of the SM. Until rather recently, Weakly Interacting Massive Particles (WIMPs) [1] and axions [2, 3] were the leading contenders for DM as their existence arises from UV-complete frameworks, such as Supersymmetry, or from attempts to address other issues, such as the strong CP problem. While the very important searches for these particles are continuing, the lack of any positive evidence for these scenarios necessitates that we widen our scope of potential DM candidates as well as the techniques to look for them [4, 5]. One scenario which is getting significant attention is the kinetic mixing/vector portal model [6, 7] wherein one posits a new dark $U(1)_D$ gauge field, the dark photon (DP), as a mediator of the interaction between DM and the SM. This interaction is generated via the kinetic mixing (KM) of this new gauge field with the SM hypercharge $U(1)_Y$ via loops of particles charged under both gauge groups and is characterized by a mixing strength parameter $\epsilon \sim 10^{-(3-4)}$ or so. For DM and DP in the $\sim 10 - 1000$ MeV range, this interaction is strong enough for the cross section of DM annihilating into SM particles to be of the right magnitude required for the DM to reach its observed abundance via the familiar freeze out (FO) mechanism, *i.e.*, the DM here is a thermal relic as in the WIMP scenario. The general parameter space of this model framework is being explored by multiple existing experiments and will be explored even further by numerous future planned experiments employing various innovative techniques [4, 5].

Extra dimensions (ED) are a useful tool for building interesting models of new physics to address outstanding issues [8]. In our earlier paper [9], hereafter referred to as I, we examined a toy 5-D version of the KM model assuming a single, flat, extra dimension [10, 11] which could be described as a bounded interval of size $R^{-1} \sim 10 - 1000$ MeV with the SM fields living on one of the brane boundaries as 4-D objects while the DM and DP experienced the full 5-D. In I, in addition to discussing the general setup for such an approach, we considered the case where the DM was a complex scalar field, S , such that the DM annihilation process was automatically a p -wave process. This easily avoids, as in 4-D, the well-known strong constraints on this cross section arising from the CMB at $z \sim 600$ [12, 13] and more recently from 21 cm measurements at $z \sim 17$ [14–16]. The p -wave nature of the annihilation process allows it to be velocity-squared suppressed at later times (due to lower temperatures) but still large enough to yield the necessary rate at FO to produce the observed DM abundance. In addition to providing new experimental signatures to search for, this framework accomplished several interesting things: *(i)* The lightest field in the DP Kaluza-Klein (KK) tower could obtain its mass via boundary conditions (BCs) without the need to introduce a dark SM singlet Higgs field which obtains a vev and spontaneously breaks the $U(1)_D$. *(ii)* The DP and DM masses are naturally of the same order $\sim R^{-1}$ without any tuning. *(iii)* The mixing of S with the SM Higgs can be negated in some cases via a choice of BCs thus avoiding potentially dangerous exotic Higgs decays; this can only be done by fine-tuning in 4-D. *(iv)* The higher KK modes of the DP were shown to necessarily decouple from the SM. Further, given the very weak coupling of the dark sector to the SM, we saw that ordinary SM physics is shielded from most of the internal dynamics of this (Abelian) dark sector even if it becomes somewhat strongly coupled at high mass scales.

In the present paper we extend our previous study to the case where the DM is a fermion. In 4-D, in such a situation, only Majorana fermions are allowed as DM since they naturally lead to a p -wave or a co-annihilation process. On the otherhand, Dirac DM annihilating via a spin-1 DP mediator is necessarily an s -wave, velocity-independent process and so is excluded by the discussion above. As we will see below, however, going to 5-D allows for a new mechanism, occurring through the destructive interference of DP KK exchanges, that can produce a sufficiently large annihilation cross section at FO while the same process is simultaneously highly suppressed at lower temperatures in a manner similar to resonant enhancement. The generalization of the 4-D Majorana DM scenario to 5-D will also be seen to bring something new. Not only do these fermions couple in an ‘off-diagonal’ manner to the DP (allowing for co-annihilation when the splitting between the mass eigenstates is small) but also a diagonal coupling term can be generated. This, as we will see, originates from the fact that the DM couplings to the DP

KK tower are generally *not* vector-like as they are in 4-D and this allows for a direct p -wave annihilation process that is effective even when the Majorana mass splitting of the DM with its heavier partner is large. Both of these fermionic model possibilities can lead to exotic signatures at the experiments that are searching for the production of DP. Of course, we remind the reader that these are only incomplete toy models at this point and should be understood as suggestive frameworks for more complete constructs. However, these successes indicate that more realistic versions of the models of the type discussed here need to be pursued.

The outline of this paper is as follows: In Section 2, we first provide a summary of the common 5-D bulk gauge and scalar physics from I that will be required in our subsequent analyses. As we will see, the detailed nature of the bulk scalar (beyond its having a vev) is mostly irrelevant to this setup as it plays no essential role in the DM annihilation or scattering processes. We then discuss the case of a SM singlet, 5-D bulk fermion with a Dirac mass as DM (Model 3) and introduce a mechanism, which is the KK generalization of the familiar resonance enhancement scenario, which would allow for s -channel DM annihilation. The required enhancement of the freeze-out annihilation cross section in comparison to that near $T \sim 0$ is shown to be of order 10^4 . The necessary conditions for this mechanism to function properly are discussed and then a scan of the model parameter space is performed to identify regions where these are satisfied so that the mechanism can be operative. The specific predictions and properties of several benchmark points having the desired properties in the relevant successful parameter region are then discussed in some detail. In particular, it is noted that the DM KK tower states generally can have parity-violating couplings to the DP gauge KK states but with a fixed coupling pattern. The DM direct detection cross section in this scenario is shown to be quite small but may be potentially observable. In this scenario, experimental DP searches for *either* e^+e^- or missing energy final states should observe signals originating from the decays of lightest two gauge KK tower modes. Section 3 contains a discussion of the case of DM being a Majorana fermion (Model 4). Here we choose the dark charge of the previously introduced bulk scalar such that it can produce a Majorana mass term after SSB which then splits the previous Dirac state into two, generally far from degenerate, Majorana states. With the lightest of these being identified as the DM, we find that co-annihilation is generally not effective in this setup due to the naturally large mass splitting. However, due to the parity-violating fermion couplings, a p -wave annihilation channel via the DM axial-vector coupling to the DP is shown to exist, something not found in the 4-D models. We again introduce a pair of benchmark scenarios to examine the details of this setup. In this model class, the elastic direct detection process is shown to be loop suppressed while inelastic scattering is kinematically forbidden due to the previously mentioned large mass splitting. The production signals for the DP KK states in this scenario are shown to be potentially more complex than in the Dirac case. Section 4 contains a Summary and our Conclusions.

2 Model 3: Dirac Fermion Dark Matter

As is well-known, and as discussed in I, data from the CMB and more recently from 21 cm measurements as discussed above, highly constrain DM annihilation into, *e.g.*, e^+e^- final states in our mass range of interest. These results exclude cross sections even remotely approaching the canonical thermal freeze-out (FO) value required to reproduce the observed relic density [17] by factors of order $\gtrsim 10^{2-4}$, with the stronger (weaker) constraint applying to lighter (heavier) DM masses. This is a particular problem if the DM annihilation is an s -wave process as in this case $\langle \sigma v_{rel} \rangle$ is roughly velocity/temperature independent so that the value at the time of FO, the CMB ($z \sim 600$), the 21 cm measurements ($z \sim 17$) and today ($z = 0$) will be essentially identical. In 4-D, in addition to excluding DM masses in excess of that of the DP (which will lead to an s -wave annihilation process with a pair of a spin-1 mediators in the final state), the choice of DM being a Dirac fermion is excluded as this annihilation process, occurring via DP exchange, is necessarily s -wave. At the very upper end of the DM range of interest to us, $\gtrsim 1$ GeV, where, *e.g.*, the CMB data alone requires that $\langle \sigma v_{rel} \rangle_{CMB} / \langle \sigma v_{rel} \rangle_{FO} \lesssim 10^{-2}$, one may be able to evade this constraint by employing a standard resonance enhancement mechanism during FO [18]. The essential idea is that at FO, the larger thermal velocities of the DM push their center of mass collision energy upwards toward the DP resonance peak (provided the DM mass relative to that of the DP is properly tuned) but then falls back to smaller values for the lower temperatures during the CMB and

later eras. However, the 21 cm constraints, taken at face value, would be roughly an order of magnitude more demanding for which the conventional resonance enhancement would be inadequate unless the DM is even more massive. Furthermore, it is clear that such a mechanism will be insufficient for satisfying the weaker CMB bound *alone* for lower DM masses of order 10 MeV or even 100 MeV. Clearly, if we want to evade these bounds for Dirac DM in this mass range some other, more powerful enhancement mechanism must be active. The fact that we are working in 5-D can provide for the existence of such a mechanism to which we now turn.

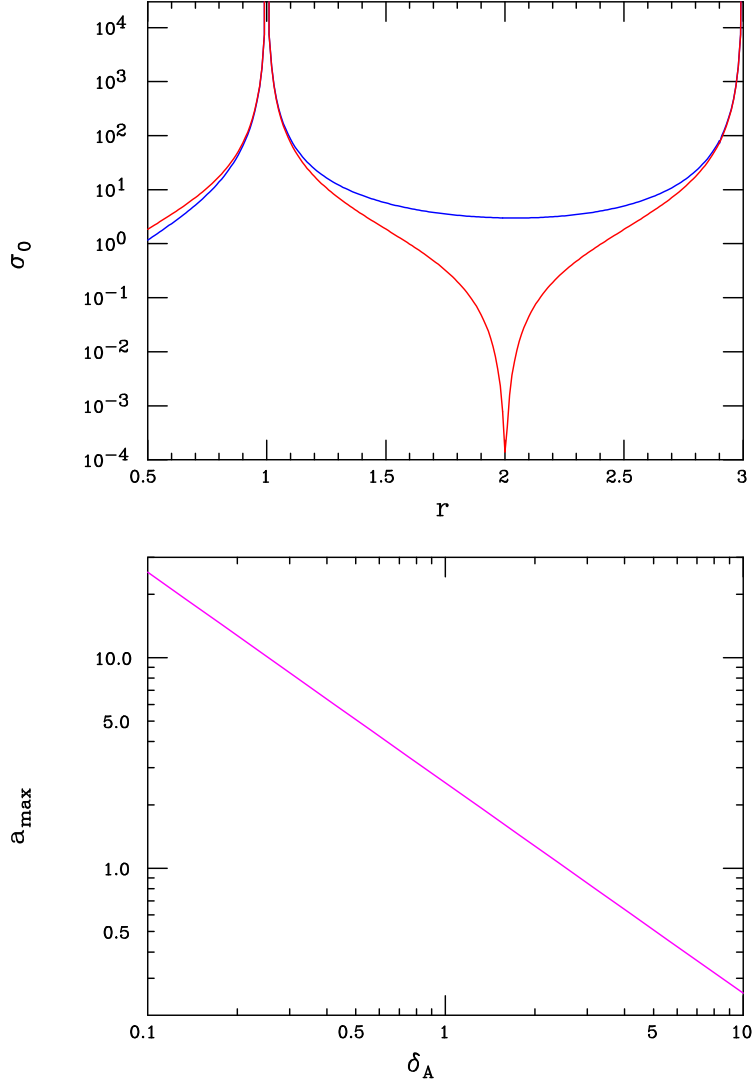


Figure 1: (Top) $T = 0$ DM annihilation cross section (in arbitrary units) in the simple toy model discussed in the text. The red(blue) curve corresponds to the case of same-sign (alternating sign) couplings. (Bottom) The upper bound on a , *i.e.*, a_{\max} as a function of δ_A in the general vicinity of $\delta_A = 1$.

To get the basic idea, we first consider two very similar versions of a simple toy model for the interaction of Dirac DM with the DP KK tower states assuming for purposes of demonstration that the magnitude of the product of the DM/SM couplings are the same for each KK level and that the DP tower masses are given by $M_{V_n}/M_{V_1} = 2n - 1$, qualitatively similar to the more realistic models to be

discussed below. Then, again qualitatively, $\sigma_0 = \sigma_{v_{rel}}$ for DM pair annihilation into SM final states as a function of $r = \sqrt{s}/2M_{V_1} \leq 3$ is given, apart from an irrelevant overall factor, in the upper panel of Fig. 1 when all of the gauge KK couplings are the identical (red) and where they have the same magnitude but alternate in sign (blue). Here we see a phenomena that has been well known since the early days of KK phenomenology: when all the couplings have the same sign there is a narrow, very strong destructive interference region lying between the first two KK resonances, which in fact, in this simple toy example lies exactly halfway between them at $r = 2$. Note that this strong destructive interference is *absent* when the sign of the couplings alternate and σ_0 behaves ‘normally’ between the first two KK resonances. Further note that when this destructive interference is present the ratio of the minimum cross section value between the two KK peaks to that at the top of the second KK peak can be as large as $\sim 10^5$ or even greater. Thus we can imagine that if we can arrange for σ_0 during the CMB/21 cm (and in the present) era to correspond to that obtained near $r = 2$ here while during FO a larger value of r is more representative due to $T \neq 0$ effects (and so σ_0 is significantly larger) then we may be able to evade the Dirac fermion s -channel cross section constraints. We will refer to this modified version of the traditional resonance enhancement setup as the KK-mechanism. Of course this simple toy model is not applicable in a more realistic situation since we know from our earlier work that, *e.g.*, amongst other factors, (i) the KK gauge masses will not be equally spaced, (ii), the relevant couplings of the DM initial state and SM final state will both vary as one ascends the gauge KK tower and will generally oscillate in sign, and that (iii) the destructive minimum must occur at smaller values of r than in the simple toy model since we still must insure that $m_{DM} < M_{V_1}$ to avoid DM pair annihilation into the $2V_1$ final state process. It is also obvious that we need to move the deep destructive interference minima closer to the second resonance peak to allow $T \neq 0$ effects to push the cross section to significantly larger values. Whether or not we can discover a set of model points in our parameter that has the necessary flexibility to achieve our desired goals while satisfying all other constraints is a non-trivial challenge. To get there we must first examine the details of the Dirac DM scenario.

Along the familiar lines as in our previous 5-D constructions, consider a setup which has the following components: a flat ED *interval* described by a co-ordinate $0 \leq y \leq \pi R$ with two 4-D branes bounding either end and with the SM living on the $y = 0$ brane. In the bulk, we have the familiar 5-D $U(1)_D$ gauge field \hat{V}^A which kinetically mixes with the SM hypercharge field, \hat{B}^μ , on the SM brane and which must have a brane localized kinetic term (BLKT) [19], described by a parameter δ_A , also on the SM brane for the reasons described in I. The bulk also contains a SM singlet, DM fermion field, X , which has a 5-D Dirac mass, m_D , and that has a dark gauge charge $Q_D(X) = 1$. A complex, SM singlet scalar, S is also present in the bulk with $Q_D(S) = Q_D$ and whose potential leads to a non-zero vev for this field, v_s . This complex scalar is not required to have a BLKT although this addition is straightforward. Note that a coupling of the form $\bar{X}XS$ is forbidden by gauge invariance so that in the 4-D theory there will be no renormalizable coupling between the Dirac fermion and scalar field towers. The full action for this scenario then takes the form

$$S = S_1 + S_2 + S_{BLKT} + S_{HS} \quad (1)$$

where the various pieces are given by

$$S_1 = \int d^4x \int_0^{\pi R} dy \left[-\frac{1}{4} \hat{V}_{AB} \hat{V}^{AB} + \left(-\frac{1}{4} \hat{B}_{\mu\nu} \hat{B}^{\mu\nu} + \frac{\epsilon_5}{2c_w} \hat{V}_{\mu\nu} \hat{B}^{\mu\nu} + L_{SM} \right) \delta(y) \right], \quad (2)$$

describes the SM plus pure 5-D gauge interaction including the KM on the 4-D brane. The hatted fields must undergo field redefinitions to bring this term into canonical form and, as usual, $D_A = \partial_A + ig_{5D} Q_D \hat{V}_A$ is the gauge covariant derivative in obvious notation.

$$S_2 = \int d^4x \int_0^{\pi R} dy \left[i \bar{X} \Gamma^A D_A X - m_D \bar{X} X + (D_A S)^\dagger (D^A S) + \mu_S^2 S^\dagger S - \lambda_S (S^\dagger S)^2 \right] \quad (3)$$

describes the bulk fermion and scalar pieces with Γ_A being the 5-D gamma matrices and

$$S_{BLKT} = \int d^4x \int_0^{\pi R} dy \left[-\frac{1}{4} \hat{V}_{\mu\nu} \hat{V}^{\mu\nu} \cdot \delta_A R \delta(y) \right] \quad (4)$$

describes the gauge BLKT term on the SM 4-D brane. Finally, the action also contains the potentially dangerous term

$$S_{HS} = \int d^4x \int_0^{\pi R} dy \lambda_{HS} H^\dagger H S^\dagger S \delta(y) \quad (5)$$

with H being the SM field, which we can either render benign as in I by choice of BCs or we can simply perform an appropriate fine-tuning of λ_{HS} as in 4-D.

With such a large compactification radius as we consider here one might have concerns that the dark sector $U(1)_D$ gauge theory may become strongly coupled before we reach the ~ 100 GeV weak scale relevant for the SM. We can use Naive Dimensional Analysis (NDA) to estimate this scale: $\Lambda_{NDA} \sim 16\pi^2/g_{5D}^2 \sim 16\pi^2/(g_{4D}^2 R)$. For a lightest gauge KK mass $m_{V_1} \sim 100$ MeV and $g_D = g_{4D} \sim 0.1$, typical of what we will deal with below, one obtains $\Lambda_{NDA} \sim 3.2 - 3.5$ TeV which is fairly safe as such large mass scales will not be remotely approached in the discussions below. Note that this scale corresponds to roughly $N_{KK} \sim \Lambda_{NDA} R \sim 10^4$ KK *levels* before the onset of strong coupling. Also, as noted in I, the SM is itself shielded from any potential dark sector strong coupling by the tiny sizes of the couplings to the more massive gauge KK states.

As described in I, after field redefinitions the gauge and scalar parts of the present Model 3 are essentially those given by Model 2, except for the interchange of the roles of the $y = 0$ and $y = \pi R$ branes, which leads to some minor changes, and the fact that the dark charge of S is here not restricted, with the bulk Dirac fermion being essentially the only new element. Given these small changes, let us briefly summarize some essential aspects of Model 2 with these differences incorporated.

The vev of the dark Higgs, S , produces a bulk mass for the dark gauge field so that masses of the corresponding KK tower fields, V_n , are given by

$$m_{V_n}^2 = \left(\frac{x_n^V}{R}\right)^2 + (g_{5D} Q_D v_s)^2, \quad (6)$$

where the roots x_n^V are found to be given by the solutions of the equation

$$\cot \pi x_n^V = \frac{\delta_A}{2x_n^V} \left[(x_n^V)^2 + (g_{5D} Q_D v_s R)^2 \right] = \Omega_n \quad (7)$$

with the useful dimensionless combination of roughly $O(1)$ factors $a = (2g_D Q_{5D} v_s R)^2$ frequently appearing in the discussions to follow. For each value of the BLKT parameter, δ_A , one finds that there is a maximum value for the parameter a , $a_{max} = 8/(\pi\delta_A)$ (and vice versa) which is shown in the lower panel of Fig. 1. This boundary is easily seen as arising from the root equation and corresponds to locations where the lowest lying gauge root is being driven to zero. If larger values of a were considered, then imaginary values for this lowest root would be obtained although physical masses for the lightest gauge mode might still be possible depending upon the specific value of a over a narrow range. This bound will play an important role in the discussion that follows as will be the flexibility to adjust the relative contributions of this bulk mass term and the ‘geometric’ piece $\sim 1/R$ to the total masses of lowest gauge KK excitations. This is so since we need to have the ratio of the masses of next to lightest to the lightest KK state to be < 2 for the KK-mechanism to work. The mass of the lightest gauge KK state as functions of both δ_A, a are shown in Fig. 2. The gauge tower 5-D wavefunctions are given by

$$v_n(y) = N_n^V \left(\cos x_n^V \phi - \frac{1}{t} \sin x_n^V \phi \right) \quad (8)$$

where we employ $\phi = y/R$ with $t = \tan \pi x_n^V = \Omega_n^{-1}$ and where the normalization is given by

$$(N_n^V)^2 = \frac{2}{\pi R} \left[1 + \Omega_n^2 + \frac{\delta_A}{\pi} - \frac{\Omega_n}{\pi x_n^V} \right]^{-1}, \quad (9)$$

so that the effective KM parameters for the gauge KK tower states are given by $\epsilon_n = \epsilon_5 N_n^V$ as before.

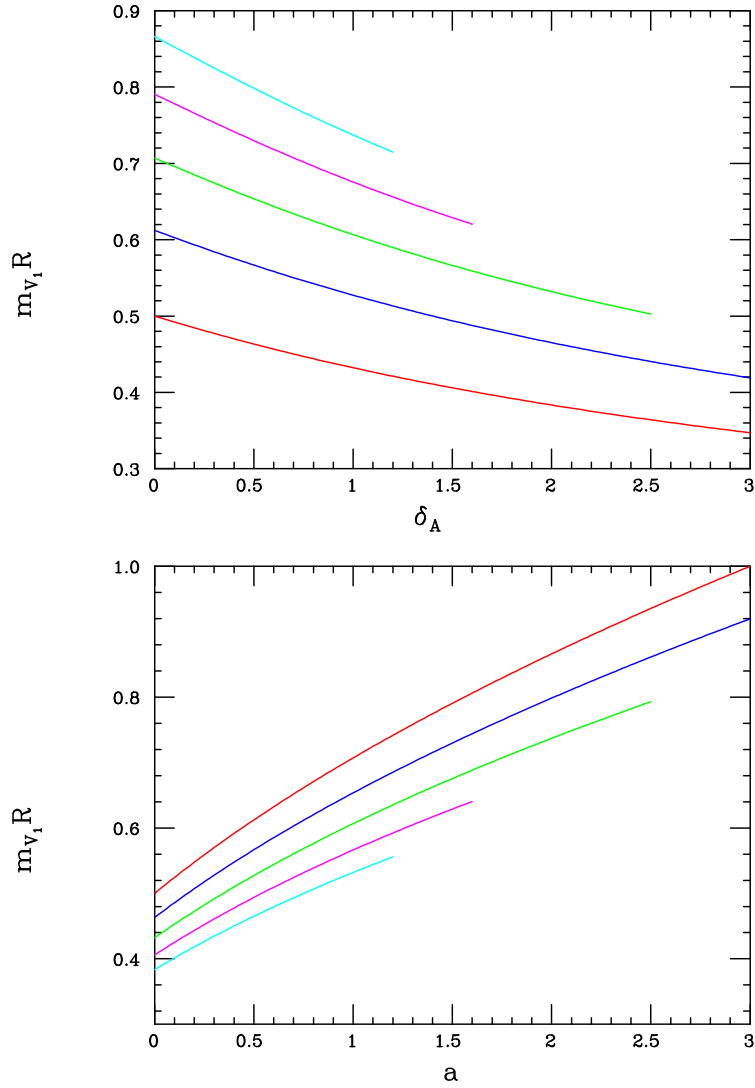


Figure 2: (Top) Lightest gauge KK mass as a function of δ_A for $a = 0(0.5, 1, 1.5, 2)$ corresponding to the red (blue, green, magenta, cyan) curve. (Bottom) Same as above but with the roles of a and δ_A interchanged. Note that that the curves terminate due to the a_{max} bound as discussed in the text.

As discussed in I, the vev of the complex scalar S splits this field into a set of CP-even fields, h_n , and a set of CP-odd fields, ϕ_n (as $S \rightarrow (v_s + h + i\phi)/\sqrt{2}$), which will in general mix with the fifth component of the gauge KK fields, V_{5n} , to form the Goldstone bosons, G_n , and a set of physical CP-odd fields, a_n . Actually, since S does not couple to the bulk fermion field X , as we will discuss below, it plays no important role in our discussion here (outside of it having a vev) and we can be quite agnostic about it as long as we insure that the lightest physical h, a KK states are more massive than the lightest fermion tower state (*i.e.*, the DM) which can easily be done by judicious parameter choices. For simplicity and to be definitive, we here follow I and employ the results in Ref. [20] although we stress that this choice isn't necessary for any of the development below. Following, *e.g.*, [20], we then have

$$\begin{aligned} G_n &= \frac{\sigma_n V_{5n} + g_{5D} Q_D v_s \phi_n}{(\sigma_n^2 + (g_{5D} Q_D v_s)^2)^{1/2}} \\ a_n &= \frac{\sigma_n \phi_n - g_{5D} Q_D v_s V_{5n}}{(\sigma_n^2 + (g_{5D} Q_D v_s)^2)^{1/2}}, \end{aligned} \quad (10)$$

where $\sigma_n = (n+1/2)/R$ ¹. Note that we shift the field S and rewrite the action in terms of h, ϕ first before applying any BCs to the solutions of the equations of motion of these fields. The Goldstone bosons are, as usual, absent in the unitary gauge in which we will work, while the a_n KK tower fields acquire physical masses that are given by [20] $m_{a_n}^2 = (\frac{n+1/2}{R})^2 + (g_{5D} Q_D v_s)^2$. The h_n masses are correspondingly given by $m_{h_n}^2 = (\frac{n+1/2}{R})^2 + 2\lambda_S v_s^2$; here the dimensionless parameter combination $h = 8\lambda_S v_s^2 R^2$ will become useful. As we will see below, unlike in I, we will concentrate on scenarios where the mass hierarchy of the lowest KK modes is given by $m_{\chi_1} < m_{V_1} < m_{h_1} < m_{a_1}$ where m_{χ_1} is the Dirac fermion DM mass. (Of course it is always possible to choose a different mass ordering of a_1 and h_1 without it having any influence on the fermion DM phenomenology we will discuss here as h, a play no important roles as discussed above.) Note that this choice of mass hierarchy requires that the ratio of parameters $h/a = 2\lambda_S/(g_{5D} Q_D)^2 < 1$ and that $m_1^V < m_1^a$ which both are easily satisfied over a large part of the parameter space. The constraint $m_{V_1} < m_{h_1}$ will place a *lower* bound on the ratio h/a ; since neither h_1 nor a_1 are to be DM, unlike in I, we can permit them to decay rather rapidly. As in I, the couplings among the dark scalars and gauge fields (in units of Q_D) are determined by the integrals over the products of the 5-D wavefunctions which takes the general form (where the $\cos \theta_m$ is the mixing factor defined above)

$$g_D \cdot c_{mn}^i = g_{5D} \int_0^{\pi R} dy \cos \theta_m a_m(y) h_n(y) v_i(y). \quad (11)$$

Note that since there will be both scalar and fermion fields coupling to the gauge KK tower in this model, it is convenient to define the 4-D gauge coupling here simply in terms of the normalization/geometric factors as

$$g_D = g_{5D} R \left(\frac{2}{\pi R} \right)^{3/2}. \quad (12)$$

We imagine for numerical calculations that $g_D \sim 0.1$ or so. We again stress that these scalars will not play any significant role in what follows outside the existence of the vev itself since they do not mediate any important interactions.

We now turn our attention to the equations of motion for the left- and right-handed components of the fermion field, X ; we will denote their wavefunctions by $f_n^{L,R}(y)$ so that the KK decomposition of X in the action above is given by

$$X = \sum_n \left(P_L f_n^L(y) \chi_n^L(x) + L \rightarrow R \right), \quad (13)$$

with P_L being the usual helicity projection operator. We recall that the success of the fermionic KK decomposition requires, from the intermediate use of integration by-parts, that these wavefunctions satisfy the coupled BC: $f_n^L f_m^R(\pi R) - f_n^L f_m^R(0) = 0$ for all n, m . This type of condition is trivially satisfied in

¹As in I, we will write these expressions in the form employing KK level dependent mixing angles: $a_n = \cos \theta_n \phi_n - \sin \theta_n V_{5n}$, *etc.*, as will be employed below.

orbifold models but this is not necessarily so in the present case. The orbifold choice is conventionally employed so as to have a chiral zero-mode which is not something we desire for DM in the present setup hence necessitating a different choice of BCs. However, just as the requirement of the absence of the Higgs portal above and in I restricted the bulk scalar wavefunction BCs, we can play a similar game with the fermion wavefunctions in order to avoid a simple neutrino portal of the form $\lambda_n^i LH\bar{\chi}_n^R$, where L^i are the three SM lepton doublets, by requiring that $f_n^R(0) = 0$ so that the χ^R cannot act as RH-neutrinos. We note that if the set of λ_n^i were to take on a common value then the limit on the invisible width of the Higgs [21] would require this value to be $< 10^{-5}$ since many KK modes of χ^R could contribute to this final state. If we chose $f_n^R(0) = 0$ to avoid this problem, then we must also have either $f_n^{L,R}(\pi R) = 0$ to fully satisfy the above by-parts BC constraint.

To move ahead, consider the coupled set of equations of motion of the fermions:

$$(\pm\partial_y - m_D)f_n^{L,R} = -m_n^F f_n^{R,L}, \quad (14)$$

where m_n^F are the physical masses of the fermion KK states. If we assume a solution of the form $f_n^R(y) = A_n \cos \sigma y + B_n \sin \sigma y$, the requirement that $f_n^R(0) = 0$ trivially leads to $A_n = 0$. Combining these two equations into a single second-order one also tells us that $\sigma = x_n^F/R$ where the values of x_n^F will be supplied by solving the appropriate root equation below so that $(m_n^F)^2 = (x_n^F)^2/R^2 + m_D^2$. Normalization of the f_n^R wavefunction on the $0 \leq y \leq \pi R$ interval further informs us that

$$B_n^2 = \frac{2}{\pi R} \frac{(x_n^F)^2 + \delta^2}{(x_n^F)^2 + \delta^2 + \delta/\pi}, \quad (15)$$

where $\delta = m_D R$. To avoid orbifold BCs and a massless zero-mode, we now assume $f_n^L(\pi R) = 0$ to satisfy the integration by-parts condition which then fully determines this set of wavefunctions to be

$$f_n^L(y) = \sqrt{\frac{2}{\pi R}} \frac{x_n^F}{\sqrt{(x_n^F)^2 + \delta^2 + \delta/\pi}} \left(\cos x_n^F \phi + \frac{\delta}{x_n^F} \sin x_n^F \phi \right), \quad (16)$$

with $\phi = y/R$ as above and also leads to the desired root equation

$$x_n^F \cot \pi x_n^F + \delta = 0, \quad (17)$$

which requires that $\delta > -1/\pi$ in order to avoid there being tachyonic roots and/or ghosts. Typical values of the smallest root and the corresponding values of the lightest fermion (*i.e.*, DM) mass as a function of δ over the interesting range are shown in Fig. 3; note that $x_1^F \rightarrow 0$ as $\delta \rightarrow -1/\pi$ below which value the tachyonic root appears. Once purely geometric factors are accounted for as in the scalar case, the coupling of these left-and-right-handed fermion tower fields to the the gauge KK tower are given by

$$g_D \cdot g_{mn}^{L,R i} = g_{5D} \int_0^{\pi R} dy f_m^{L,R}(y) f_n^{L,R}(y) v_i(y). \quad (18)$$

Note that, in all generality, $g_{mn}^{L i} \neq g_{mn}^{R i}$ so that the interaction of the DM with the DP tower is potentially *parity-violating*. This result is initially puzzling until one recalls that this happens to the lowest fermion mode all the the time in conventional orbifold models since there either f_0^L or f_0^R is *absent* by construction in order to obtain a massless mode and which is seen to be *maximally* parity/charge conjugation violating. Of course in such models the higher fermion modes will have a vector-like coupling but that will not be the case here although definite patterns in the KK tower couplings do appear; some details of these couplings will be discussed below. We remind that here the state $\chi = \chi_1$ is to be identified with the DM²

Summarizing, apart from the overall mass scale set by R^{-1} , Model 3 is described by 4 parameters: δ_A, a, δ and h which determine all the masses and couplings amongst the various KK states. While the gauge KK mass spectrum is controlled by δ_A, a alone, their couplings to DM also depend upon δ . h will play no role in what follows. We note that as a becomes larger the lower end of the gauge KK spectrum

²Note that, as usual, heavier dark sector fermion fields can be added if needed to cancel any induced gauge anomalies.

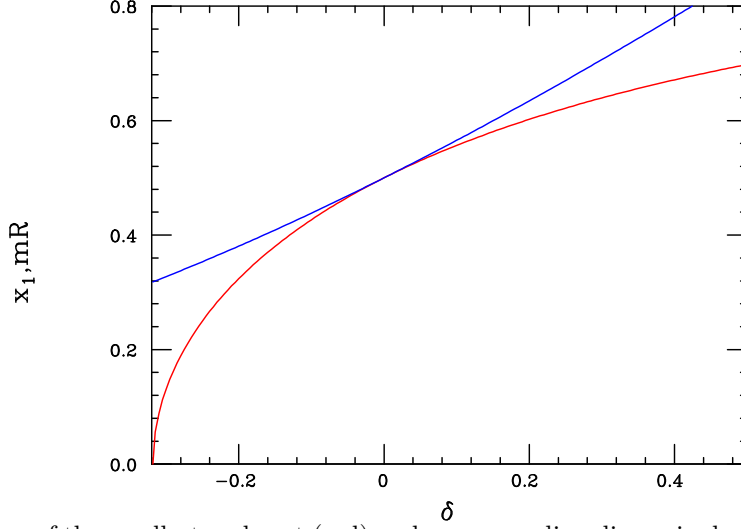


Figure 3: The value of the smallest real root (red) and corresponding dimensionless DM mass as functions of δ .

will become more compressed as the dominant parts of the masses are arising from the Higgs vev and not the size of the interval. Thus for a given value of δ_A , values of a not too far from a_{max} will likely be the most interesting for us. Similarly, positive values of δ , yielding larger masses for the DM relative to the gauge KK states will likely prove the most interesting. We now perform a scan over these three parameters assuming the following ranges: $0.1 \leq \delta_A \leq 3$, $0 \leq a \leq a_{max}(\delta_A)$, and $-1/\pi \leq \delta \leq 1.5$ while simultaneously imposing the requirements that (i) the DM mass is below that of the lightest gauge KK state, (ii) the product of the SM and DM couplings to the lightest two gauge KK states have the same sign and with the ratio of the DM vector coupling of the second gauge KK state to that of the lowest state $\gtrsim 0.5$ to maximize destructive interference, (iii) $0.5m_2^V \leq 2m_{DM} \leq 0.98m_2^V$ while also $2m_{DM} \geq 1.4m_1^V$. These requirements will push the mass spectra and couplings towards the parameter space regions where the likelihood of the KK-mechanism being active are the most the probable. Since this is a zero-temperature calculation we next examine the surviving points to see whether or not they produce suppressed values of the annihilation cross section indicative of the strong destructive interference we are seeking. Assuming this set of points is non-empty, we then extract a set of benchmarks (BMs) that will suggestively show the type and scale of the possible variations within this allowed space and calculate the ratio, K , of their finite temperature ($x_F = m_{DM}/T = 20$ is assumed here) thermally averaged annihilation cross sections at FO to their corresponding values of the zero-temperature ($T = 0$) annihilation cross section. Recall that we will require that $K \gtrsim 10^4$ for this result to be interesting.

The cross section for $\chi\bar{\chi} \rightarrow e^+e^-$ (e^+e^- being a stand-in here for all of the light, kinematically accessible SM states) in the $m_e \rightarrow 0$ limit is given by

$$\sigma = \frac{\alpha g_D^2 \epsilon_1^2}{3\beta_\chi s} \sum_{ij} P_{ij} \frac{\epsilon_i \epsilon_j}{\epsilon_1^2} \left[v_i v_j \frac{3 - \beta_\chi^2}{2} + a_i a_j \beta_\chi^2 \right] \quad (19)$$

where the sum extends over intermediate vector KK tower fields, V_i , $\epsilon_i/\epsilon_1 = N_i^V/N_1^V$, which for our BMs that we will discuss is shown in Fig. 4, $\beta_\chi^2 = 1 - 4m_\chi^2/s$, $(v_i, a_i) = \frac{1}{2}(g_{11}^{L\ i} \pm g_{11}^{R\ i})$ (with these coupling factors not to be confused with the gauge KK wavefunctions) and

$$P_{ij} = s^2 \frac{(s - m_{V_i}^2)(s - m_{V_j}^2) + \Gamma_i \Gamma_j m_{V_i} m_{V_j}}{[(s - m_{V_i}^2)^2 + (\Gamma_i m_{V_i})^2][i \rightarrow j]} \quad (20)$$

BM	δ_A	a	δ	N	m_{V_1}	m_{V_2}	m_{DM}	Sum	$K/10^4$	r_{min}
1	1	2.42	0.235	0.342	0.784	1.495	0.659	1.125	6.38	0.604
1'	1	2.27	0.235	1.003	0.767	1.480	0.659	1.080	1.37	0.598
2	0.5	3.82	0.355	0.464	1.007	1.666	0.747	1.147	4.36	0.800
3	1.5	1.61	0.180	1.518	0.642	1.380	0.620	1.027	3.20	0.402
4	0.4	4.65	0.395	3.650	1.108	1.741	0.777	1.196	1.39	0.842

Table 1: Parameters and general properties of the five chosen Dirac DM BM models; all masses are given in units of R^{-1} .

with Γ_i being the total width of the KK state V_i . All of these quantities will be calculable within our set of chosen BMs below. For concreteness, the $T = 0$ cross section, for which $s = 4m_{DM}^2$, is given numerically by

$$\langle \sigma v_{rel} \rangle_{T=0} = 2.8 \cdot 10^{-30} \text{cm}^3 \text{s}^{-1} \text{N} \frac{(\text{g}_D \epsilon_1 / 10^{-5})^2}{(m_{V_1} / 100 \text{ MeV})^2} \quad (21)$$

where N is a roughly $O(1)$ number depending upon the specifics of the BM point. Here we see that is easy enough to satisfy both the CMB and 21 cm constraints by, *e.g.*, choosing small values of the product $\text{g}_D \epsilon_1$; the real issue is whether or not we can obtain parameter points where K is also simultaneously sufficiently large so as to obtain the observed relic density.

Fortunately, for $0.4 \lesssim \delta_A \lesssim 1.5$, we do find parameter space points satisfying all of our requirements and generally with values a not too far below a_{max} as expected. For example, when $\delta_A = 1(1/2, 3/2)$ the range of a values which produce potentially ‘interesting’ model points is roughly $2.27(3.82, 1.61) \lesssim a \lesssim 2.54(4.25, 1.69)$ with some values clearly preferred over others. These ranges are found to produce relatively deep destructive minima in the $T = 0$ cross section which are also not far below the position of the second resonant peak. To get a feeling for this parameter space, we choose the five representative BM points with a spread of parameter values and whose detailed properties are shown in Table 1. Amongst other things, we note that all of these BM points lead to values N above which are not far from unity as expected and produce values of K in excess of 10^4 as required. Now let us investigate these points a bit more closely. To do this we perform the following exercise: recalling that all of the DM couplings to the KK tower gauge fields are dependent of the DM mass itself we *freeze* these couplings to their specific BM values and explore how the kinematics of the various observables of interest depend upon the ratio $r = 2m_{DM}/m_{V_1}$; all other parameters in each BM are held fixed while this analysis is performed. The top panel in Fig. 5 shows, apart from a common overall factor, the $T = 0$ DM annihilation cross section as a function of r for our five BMs. This is the more realistic version of the simple toy model result shown in the top panel of Fig. 1 All BMs show a common first resonance peak due to V_1 but their detailed behaviors differ for larger r values due to their different mass spectra (*e.g.*, the mass of V_2 which we see as the second resonance peak) and multiple coupling variations. However, all these BMs have strong destructive minima in the required range $r < 2$, specifically, $1.41 \lesssim r \lesssim 1.94$ with the corresponding V_2 peak lying not far above this minima with a typical separation $\Delta r \simeq 0.2$ in all cases. This is far below the value of $\Delta r = 1$ seen in the simple toy model above. This small separation is a key ingredient for the success of these models since the greater temperatures at FO are limited as to how much higher they can push the DM collision center of mass energy.

The lower panel in Fig 5 shows the ratio of DM annihilation cross sections at FO to those at $T = 0$, K , as a function of r , performing the same type of analysis as in the top panel, *i.e.*, freezing all other parameters and simply varying r . Here we see several things: (i) below the V_1 peak we see the conventionally expected resonant enhancement of $K \sim 80$ which, as discussed above is insufficient for our present goals. (ii) For larger r we see the KK-enhancement peaks associated with the deep troughs in the top panel. In all cases, the actual K value at the peak is somewhat *larger* than in our chosen BMs indicating that the parameters for these representative points are not completely optimal in maximizing the value of K . However, in all cases we see that values of $K \sim 10^4$ are relatively easy to obtain employing this mechanism. To understand the importance of the relative signs of the couplings of $V_{1,2}$ to the DM, we show in Fig. 6 the same results for K as in Fig. 5 for BM1 and BM4 but now comparing to to the same

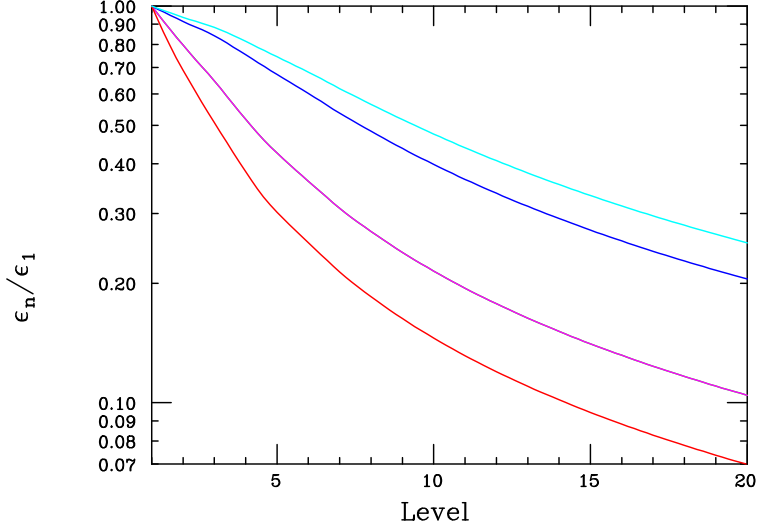


Figure 4: Values of ϵ_n/ϵ_1 appearing in the cross sections as a function of the KK level n for BM1/BM1' (magenta), BM2 (blue), BM3 (red) and BM4 (cyan).

BMs after flipping the signs of the V_2 couplings. We first see that the normal resonance enhancement below V_1 is insensitive to this coupling choice as it should be. However, when this coupling sign is flipped, we see that the very large K values for our BMs $\sim 10^{4-5}$ are reduced to values of $K \sim 30 - 40$ that might be obtained by ordinary resonance enhancement thus demonstrating the need for both $V_{1,2}$ to have the same sign couplings to obtain large K values.

Along these same lines we can immediately evaluate the $\chi(\bar{\chi}) - e$ elastic scattering cross section for our BMs, which is given generally (but in the limit of vanishing DM velocities) by

$$\sigma_e = \frac{4\alpha\mu^2 g_D^2 \epsilon_1^2}{m_{V_1}^4} \left[\sum_i \frac{\epsilon_i}{\epsilon_1} v_i \frac{m_{V_1}^2}{m_{V_i}^2} \right]^2 \quad (22)$$

where $\mu = m_e m_\chi / (m_e + m_\chi)$ is the reduced mass $\sim m_e$ for the DM masses of interest to us. Note that apart from a common overall factor, all of the BM dependence lies in the squared sum within the bracket so that, numerically, we have

$$\sigma_e = 3.0 \cdot 10^{-42} \text{cm}^2 \left(\frac{100 \text{ MeV}}{m_{V_1}} \right)^4 \left(\frac{g_D \epsilon_1}{10^{-5}} \right)^2 \times \text{Sum} \quad (23)$$

where ‘Sum’ denotes the squared summation above and whose values (also found to be close to unity due to the rapid convergence of the series) for the BM points are given in Table 1. We note here that the typical values we obtain for this cross section are a factor of order $\sim 20-50$ below the projected sensitivity of the first full incarnation of, *e.g.*, SENSEI [22–24], but may eventually be reached by experiment.

Turning to the mass spectra themselves, the requirements to obtain large K values pushes us into a relatively constrained location in parameter space which essentially determines the decay properties of the lowest lying members of the DP KK tower. Since the DM must be relatively heavy in comparison to V_1 , V_1 must *necessarily* (unlike in Models 1 and 2) decay to SM particles, *e.g.*, e^+e^- in the the mass range of interest to us. The next heavier gauge KK state, V_2 , is necessarily more massive than $2m_{DM}$ and since, $g_D^2 \gg (e\epsilon_2)^2$, essentially only decays to DM pairs. Thus V_1 is like the DP being searched for at HPS [26] while V_2 is more like the state decaying to missing momentum/energy which would be

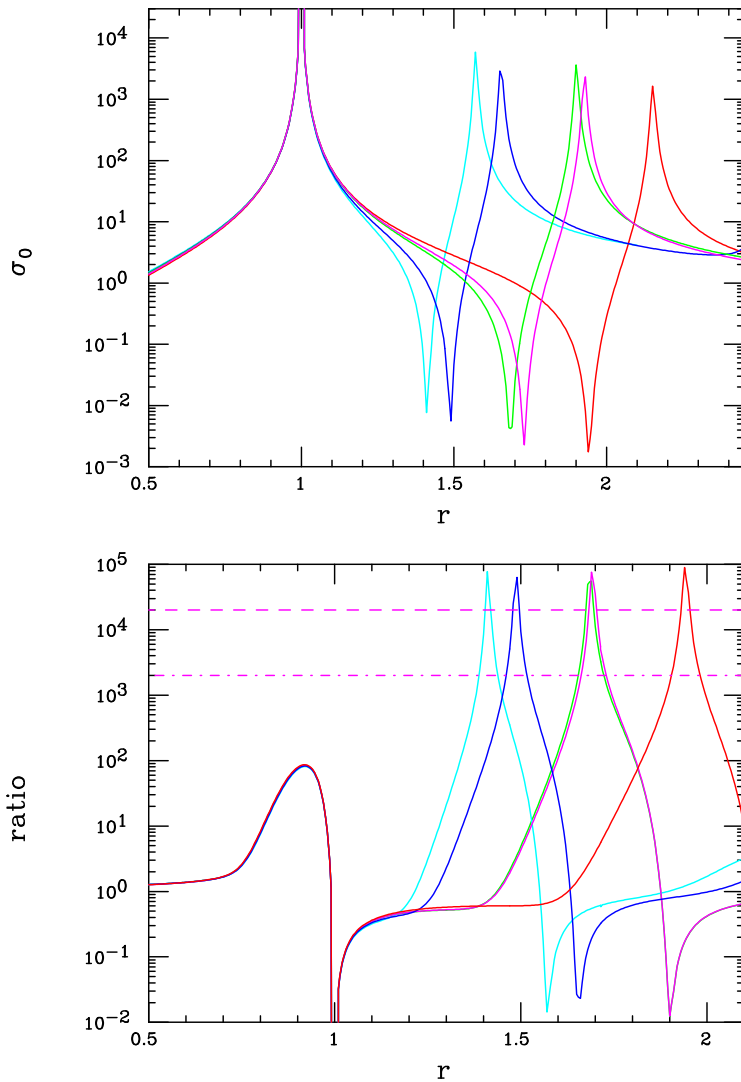


Figure 5: (Top) Scaled $T = 0$ DM annihilation cross section as a function of $r = 2m_{DM}/m_{V_1}$ for the benchmark models BM1 (green), BM1' (magenta), BM2 (blue), BM3 (red) and BM4 (cyan). (Bottom) Ratio of the freeze-out to $T = 0$ DM annihilation cross sections, K , as a function of r for the same BMs as in the top panel. The horizontal dashed (dash-dotted) lines are guides to the eye for $K = 2 \cdot 10^4$ ($2 \cdot 10^3$).

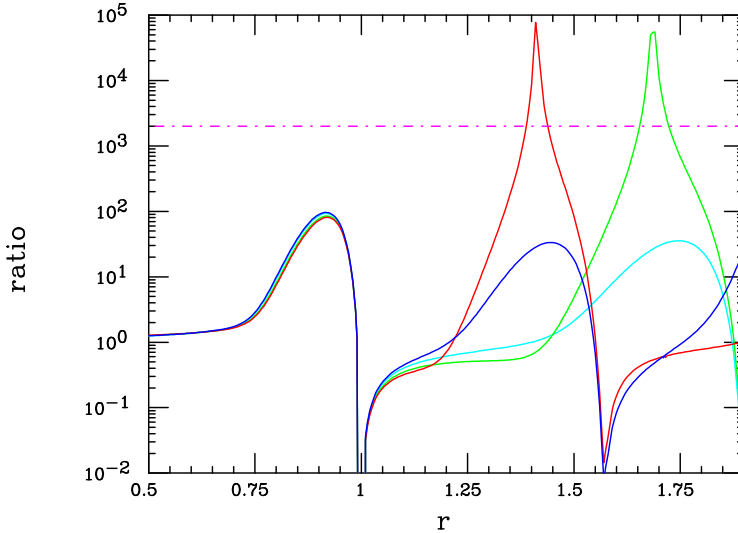


Figure 6: Same as in the lower panel of the previous Figure for BM1 (green) and BM4 (red) but also for these same BM (in cyan and blue, respectively) where we artificially flip the signs of the product of couplings of the SM and DM to V_2 for comparison. The horizontal dash-dotted line is a guide to the eye for $K = 2 \cdot 10^3$.

sought by LDMX [27]. As we'll discuss, the heavier gauge KK states will likely have more complex decay patterns.

What are the other properties of these BMs? Given the values in Table 1 the only parameter remaining unspecified (and which played no role in the above discussion) is h or perhaps more usefully the ratio $r_{ha} = h/a$ which determines the relative h_n and a_n spectra. An important aspect of the scalar sector, as noted above, is that h, a do not interact directly with the χ' s without mediation by the vectors, V . Of course there is some significant flexibility here as the h, a are essentially decoupled from the considerations above but we will employ the spectrum assumptions made earlier for purposes of demonstration; other mass spectra will lead to qualitatively similar results. One of the first issues we need to address is the manner in which h, a might decay; the possibilities are clear once we recall that the relevant interaction is of the off-diagonal form haV with possibly the most interesting situation involving the lightest KK mode in each tower. Since a_1 is assumed to be the most massive of the lowest KK levels by construction, it decays as $a_1 \rightarrow hV_n^*$, $V_n^* \rightarrow e^+e^-$ and, since by assumption $m_{h_1} > m_{V_1}$, then $h_1 \rightarrow V_1V_n^*$. Note that this mass ordering requires a different minimum value of r_{ha} , *i.e.*, r_{min} , for each BM point; these are given in Table 1. This general type of $h_iV_jV_k$ off-diagonal coupling is generated through the dark Higgs vev since only part of the masses of the gauge fields arise from this source and the mass and coupling matrices are thus not simultaneously diagonalizable. The decays of h_1, a_1 thus lead to rather complex final states with up to three pairs of e^+e^- , at least one of which is on-shell (by construction) arising in the case of h_1 decay. Since the $a_1 - h_1$ splitting can be accidentally small it is possible that the a_1 is long-lived in a situation parallel to that seen in I. As the KK towers are ascended rather complex decay patterns can be encountered; level-by-level as n increases so does the mass degeneracies between the χ_n, a_n and h_n states while the V_n generally remain somewhat lighter due to the BLKT. This large- n behavior is found to be independent of the details of scalar sector unless it too has a BLKT.

A sample spectrum for BM1 is shown in the upper panel of Fig. 7 assuming $r_{ha} = h/a = 0.8 > r_{min}$ for purposes of demonstration; the states are the *least* degenerate in the case of the lowest tower states. These mass spectra can then be used to determine which decay modes are open for the various KK tower states. For example, for this BM, we see that the following on-shell decays are kinematically accessible:

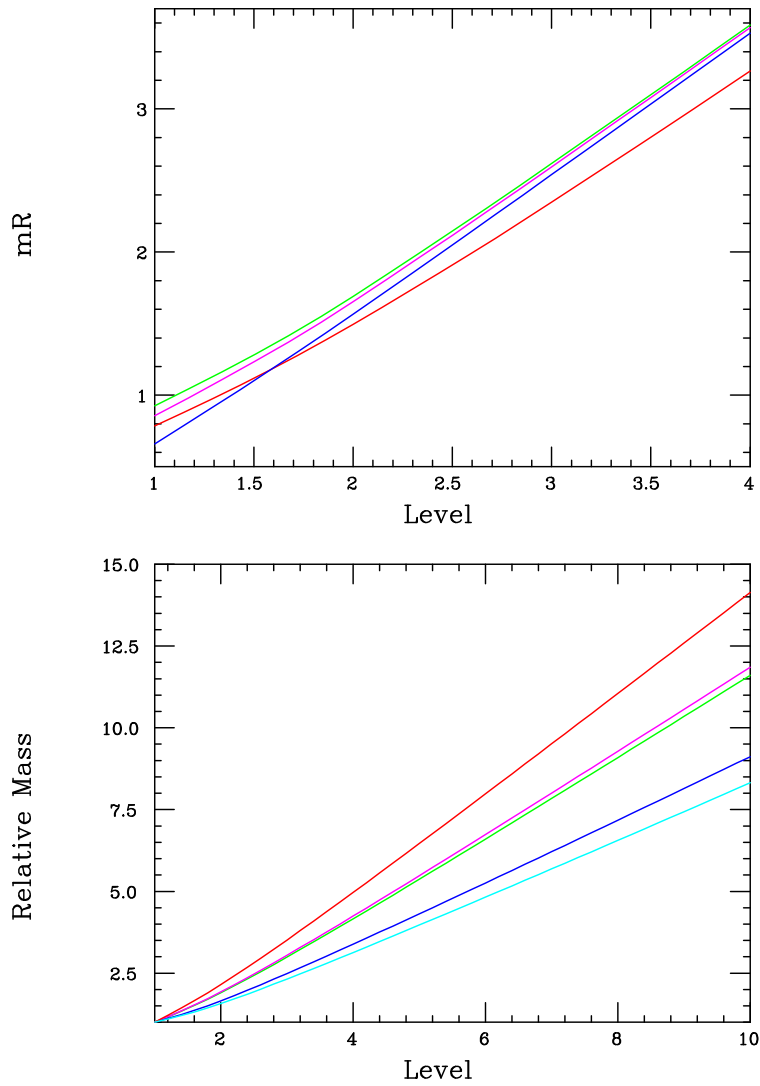


Figure 7: (Top) Mass spectrum of BM1 for $r_{ha} = h/a = 0.8$ as a function of the level n in units of R^{-1} for V_n (red), χ_n (blue), a_n (green) and h_n (magenta), respectively. (Bottom) Growth in the mass ratio m_{V_n}/m_{V_1} as a function of n for BM1 (green), BM1' (magenta), BM2 (blue), BM3 (red) and BM4 (cyan).

$V_3 \rightarrow h_1 a_1, \chi_1 \bar{\chi}_1, \chi_1 \bar{\chi}_2 + \text{h.c.}$, $a_3 \rightarrow V_1 h_1, V_1, h_2, V_2 h_1$ and $h_3 \rightarrow V_1 a_1, V_1, a_2, V_2, a_1$ while $\chi_2 \rightarrow \chi_1 V_1$ and $a_2 \rightarrow V_1 h_1$ are the only ones allowed. In this BM case, h_2 still only decays off-shell, here to $V_1 V_n^*$ and is likely long-lived. For the other BMs the set of allowed decays can be somewhat different particularly due to the gauge KK mass spectrum differences which are quite sensitive to choices of δ_A, a . In the lower panel of Fig 7 we can see how the spacing between the different gauge KK levels, m_{V_n}/m_{V_1} , grows with n for the different BMs. This shows a variation of almost a factor of $\sim 80\%$ implying that the details of the mass spectra for the different parameter space points can vary significantly. More generally, we also find the following coupling patterns for the DM tower fields for all the BMs: the DM couplings to the KK gauge tower alternate in sign after the first two gauge levels. More massive fermion KK excitations generally have parity-violating couplings to the DP. However, eventually they begin to alternate between almost pure vector (axial-vector) all with the same sign, opposite to that for the DM, for odd (even) KK levels making the KK tower couplings, asymptotically, parity-conserving.

3 Model 4: Majorana Fermion Dark Matter

The Majorana scenario can be obtained by a direct augmentation to the discussion of Dirac fermions presented in the last Section. To some extent the Majorana fermion case is simpler than the Dirac case since the DM annihilation process is now automatically p -wave if axial-vector couplings to the DP KK states exist or involves co-annihilation with its heavier Majorana partner that arises from the splitting of an originally Dirac fermion into two Majorana components. This means that we are no longer constrained to live near the DM annihilation cross section minima when $T = 0$ as in the Dirac case above thus leaving much greater parameter freedom in the gauge sector. However, it is also simultaneously *more* complex than the Dirac case since there are now 5 distinct KK towers of fields to deal with although h, a will still play almost no role here. We arrive at this scenario by returning to Model 3 above and choosing the bulk scalar to have $|Q_D| = 2$ so that it can generate a Majorana mass when S gets a vev, *i.e.*, $m_M = y_D v_s / \sqrt{2}$, via the new piece in the action:

$$S_{Maj} = \int d^4x \int_0^{\pi R} dy \left[-y_D \bar{X} X^c S + \text{h.c.} \right] \quad (24)$$

where y_D is a dark Yukawa coupling, a new free parameter which we can trade for the Majorana mass itself $m_M = \delta_M / R$. This new mass term then alters the fermion KK equations of motion above to [28]

$$(\pm \partial_y - m_D) f_n^{L,R} = -(m_n^F - m_M) f_n^{R,L}, \quad (25)$$

whose solutions are essentially identical in form to those obtained in the Dirac case above especially as we impose the same BCs on the solutions: $f_n^R(0) = 0$ and $f_n^L(\pi R) = 0$ although the mass eigenstate structure is different. Here each Dirac mass state in the KK tower is split in two with the values $m_{1,2n} R = [(x_n^F)^2 + \delta^2]^{1/2} \pm \delta_M > 0$ where x_n^F and δ have been defined above. Here, a certain parameter hierarchy and Majorana mass sign convention has been assumed, $\delta_M \geq 0$, so that physical Majorana tower masses $m_{1,2n}$ are also positive. So, *e.g.*, taking $\delta = \delta_M = 0.1$ we find the lowest Dirac KK mass to be $\simeq 0.565/R$ from Fig. 3 and hence the lowest KK values for the split Majorana states to be $m_{1,2}$ are $\simeq 0.465/R$ and $0.665/R$, respectively. Note that this is a sizable mass splitting between these two states, *i.e.*, $(m_2 - m_1)/m_1 \simeq 0.43$ and a parameter tuning would be necessary to obtain smaller values of order only a few per cent. Given the equations of motion above, the $f_n^{L,R}(y)$ reduce to the same functions as before when written in terms of x_n^F and δ and so the couplings $g_{mn}^{L,R}$ above are also completely determined once the gauge KK wavefunctions are known. However, the Majorana mass eigenstates are now just the linear combinations $\chi_{1n} = (\chi_n^L + \chi_n^R)/\sqrt{2}$ and $\chi_{2n} = i(\chi_n^R - \chi_n^L)/\sqrt{2}$, respectively³.

Suppressing Lorentz and KK indices for the moment and recalling that generally $g^L \neq g^R$ in the present setup, the interaction of the χ 's with V can be symbolically written as $g_D [(g^L \bar{\chi} \chi_L + L \rightarrow R) - \text{c.c.}] V$

³It is sometimes convenient to write these in the familiar χ, χ^c basis [25]; then $\chi_n = (\chi_{1n} + i\chi_{2n})/\sqrt{2}i$ and $\chi_n^c = -(\chi_{1n} - i\chi_{2n})/\sqrt{2}i$ as we will generally do here.

so that in terms of the mass eigenstates $\chi_{1,2}$ this becomes (still suppressing KK indices)

$$g_D \left[\frac{(g^R - g^L)}{2} (\bar{\chi}_1 \gamma_\mu \gamma_5 \chi_1 + \bar{\chi}_2 \gamma_\mu \gamma_5 \chi_2) + \frac{i(g^R + g^L)}{2} (\bar{\chi}_1 \gamma_\mu \chi_2 - \bar{\chi}_2 \gamma_\mu \chi_1) \right] V^\mu, \quad (26)$$

which we see *differs* from the 4-D case, where $g^R = g^L$ occurs naturally, since both ‘diagonal’ and ‘off-diagonal’ gauge couplings are generally obtained. In the 4-D case only the second term exists due to the purely vectorial coupling present there so that the DM reaches FO only via co-annihilating with its somewhat heavier partner. Here, we might expect this reaction to be rather suppressed in the present case due to the typically rather large mass splitting between these two states as noted above. However, a new direct process can now exist but it is p -wave (hence v^2) suppressed due to the axial-vector nature of the relevant coupling; of course this is exactly what we want in order to satisfy the CMB and 21 cm constraints. The annihilation cross section into e^+e^- in the present model is thus in the same form as Eq.(19) above but with the $v_i \rightarrow 0$ and an additional overall factor of 2 due to the Majorana nature of the DM, *i.e.*, $a_i^2 \rightarrow \frac{1}{2}(2a_i)^2$. This pair of interactions also has an immediate implications for direct detection searches for DM: in 4-D at tree-level only the inelastic process, *e.g.*, $\chi_1 e \rightarrow \chi_2 e$ is available and the two masses must be highly degenerate to obtain the observed relic density thus implying that there’s a chance that this process might occur. The elastic scattering process $\chi_1 e \rightarrow \chi_1 e$ also *does* occur but only at 1-loop in the limit of $v_{DM}^2 \rightarrow 0$. In 5-D the inelastic scattering process is unlikely to be of much relevance due to the generally large mass splittings that are expected while the new axial-vector coupling of the DM to the DP gauge tower allows for elastic scattering. However, this is found to be v^2 suppressed making it likely unobservable today. Note that the calculation of the couplings $g_{mn}^{L,R}$ follows the same path as in the case of Dirac fermions and remains only dependent upon the three parameters δ_A, a and δ and are independent of the Majorana mass parameter δ_M which only influences the Majorana mass spectrum itself.

Unlike in the Dirac case, the presence of the Majorana mass term generates an interaction between the $\chi_{1,2}$ KK states and those arising from the decomposition of the scalar S , *i.e.*, h, ϕ with ϕ then generally mixing as above with V^5 to form the physical state a and the Goldstone bosons (which we ignore). Thus S_{Maj} written in the h, ϕ basis (but with KK indices suppressed) is just

$$S_{Maj} = \int d^4x \int_0^{\pi R} dy - \frac{m_M}{v_s} \left[(\bar{\chi}_2 \chi_2 - \bar{\chi}_1 \chi_1) (v_s + h) + i (\bar{\chi}_2 \gamma_5 \chi_2 - \bar{\chi}_1 \gamma_5 \chi_1) \phi \right]. \quad (27)$$

In 4-D, an interaction of this type would possibly allow for DM annihilation to SM fields via h mixing with the SM H but this is absent here due to the BCs assumed above⁴. Of course, for other choices of the scalar BCs we would need to tune λ_{HS} to tiny values which we could always do as in 4-D. Here, above the lowest KK modes, S_{Maj} can provide new decay paths for heavier states as we will return to shortly. Also, in 4-D, the field ϕ is absent from the physical spectrum as it alone plays the role of the Goldstone boson since V^5 is absent there while here the general combination, a , survives as a physical field. However, outside of the presence of the vev, as we have seen, the h, a fields play no important role as far as the dynamics of DM is concerned as they either do not couple to the SM or they have couplings which are very highly suppressed. For the lightest KK levels if we imagine that, as above, $m_{V_1} < m_{h_1}, m_{a_1}$, then h_1, a_1 can decay as in the previous Section and this can always be arranged by judicious parameter choices. We still must require that $m_{\chi_{1,1}} < m_{V_1} < 2m_{\chi_{1,1}}$ to prevent the s -wave DM annihilation into V_1 pairs and so that the lightest gauge mode decays to the SM, *i.e.*, $V_1 \rightarrow e^+e^-$. On the other hand, V_2 will have a large (possibly dominant) branching fraction into DM pairs, similar to what we saw above in the Dirac case with the obvious implications for the experiments hoping to produce DP directly. However, the V_2 decay to DM plus its heavier Majorana partner is also possible, depending upon the exact details of the spectra, but this is seen to occur for our chosen BM points. In such a case V_2 decay will yield an e^+e^- pair as well as missing energy, something quite different than in the 4-D models. Note that there remains some freedom in the relative position of $\chi_{2,1}$ in the mass spectrum. However, its only allowed decay path (since the scalar couplings are ‘diagonal’) is via $\chi_{2,1} \rightarrow \chi_{1,1} V_1$ where it is

⁴As noted in the previous Section, the KK modes of V^5 do not couple to the SM brane-localized fields.

BM	δ_A	a	h	δ	δ_M	m_{V_1}	$m_{\chi_{1,1}}$	$m_{\chi_{2,1}}$	m_{h_1}	m_{a_1}	m_{V_2}
1	1	1	0.9	0.1	0.1	0.607	0.465	0.665	0.673	0.707	1.389
2	0.5	0.5	0.4	0.2	0.15	0.567	0.484	0.784	0.602	0.612	1.432

Table 2: Parameters of the two Majorana DM BM models; all masses are given in units of R^{-1} .

likely that the V_1 is off-shell (unless δ_M is of sufficient magnitude) so that several of these lowest mass KK states can be long-lived. Fig. 3 and Fig. 6 can be consulted to address this issue as the rather strong requirement for an on-shell V_1 decay is that $2\delta_M > m_{V_1}R$. Clearly as δ increases the value of δ_M will also need to increase to insure that the DM mass lies below that of V_1 .

Let us consider the following two sample BM points shown in Table 2 which are (essentially) random places in this rather large parameter space. In units of R^{-1} the masses of the lowest KK excitations in these particular cases are also supplied in the Table. Note that there is nothing particularly special about these points other than they satisfy the rather loose constraints discussed above; a detailed examination of the full five-dimensional parameter space would undoubtedly be a useful exercise. The fractional mass splitting between the two lightest Majorana states is seen to be sufficiently large so as to make the co-annihilation mechanism inefficient. One observes that $2m_{DM}$ lies safely away from both $m_{V_{1,2}}$, essentially at the beginning of the relatively flat cross section region between these two resonances similar to the blue curve shown in the upper panel of Fig. 1. Thus, if we ignore any co-annihilation contributions due to the large Majorana mass splitting (as well as any potentially very highly suppressed h exchanges), we may safely use the familiar expansion $\langle \sigma v_{rel} \rangle = bv_{rel}^2$ as well as the machinery for the calculation of the annihilation cross section in the previous Section as the DM annihilation process is dominantly s -channel via V_n exchange. This then yields the estimates (again assuming that $x = m_{DM}/T = 20$)

$$\langle \sigma v_{rel} \rangle = 1.2(0.74) \cdot 10^{-25} \text{cm}^3 \text{s}^{-1} \frac{(\text{gD}\epsilon_1)^2/10^{-7}}{(m_{V_1}/100 \text{ MeV})^2} \quad (28)$$

for BM1(BM2) which are not parametrically far from the value needed to obtain the observed DM relic density. Other possible BM choices lead to similar results up to $O(1)$ factors due to variations in the fermion and gauge mass spectra and the corresponding KK effective couplings.

4 Summary and Conclusions

In this paper we have considered an extension of our previous study of the 5-D kinetic mixing/vector portal model to the case where the DM is fermionic. In these setups the SM singlet bulk Higgs sector plays very little role beyond its having a vev. Unlike in the previously examined scenario of complex scalar DM, the annihilation process for Dirac fermions via a spin-1 mediator is necessarily s -wave and so is not considered in 4-D models of this type. However, in 5-D, we have examined a new mechanism which allows for this possibility which is the KK generalization of the usual resonance enhancement picture. In that setup, the mass difference $M_{res} - 2m_{DM}$ is sufficiently small so that the thermal motion of the DM near freeze-out is great enough as to push $\sqrt{s} \sim M_{res}$ which greatly increases the annihilation cross section at freeze-out. Thus the annihilation cross section can then be smaller by a factor of $K \sim 100$ when $T \sim 0$. This enhancement is insufficient in the case of the Dirac DM in the mass range of interest to us as the ratio of the required thermal cross section and the constraints from the CMB and 21 cm data is required to be of order $K \sim 10^4$. To attain such a large ratio we need not only a significant enhancement on resonance but also a strong destructive interference below, but not too far away from, the resonance where the $T \sim 0$ DM annihilation takes place. The effectiveness of this arrangement places quite stringent requirements on the DM mass and the DP KK tower spectra as well as the SM/DM-DP couplings which must be of the same sign and of similar magnitude for the first two gauge KK levels. Fortunately, in the setup we consider, these quantities were found to be controlled by only 3 parameters. A scan of this parameter space was performed and successful regions satisfying our requirements were identified resulting in the 5 sample benchmark models that we then examined in greater detail. These

BMs were found to yield K values in the range $1.4 \leq K/10^4 \leq 6.4$ and it was further shown that even larger values could be obtained with some further tuning of the parameters. All of these points led to very similar predictions for the DM-electron scattering cross section. In such a setup, DP production signals in both the e^+e^- and missing energy/momentum channels should be expected from the decays of the lightest two gauge KK states while more exotic decay signatures were possible from the other KK states.

When the DM is a Majorana field in 4-D, the DM achieves the required relic density via the co-annihilation with its somewhat more massive Majorana partner; this splitting is achieved via a coupling to a SM singlet scalar whose dark charge is chosen so that it can generate a Majorana mass term, a Dirac mass term for the DM already being present. Since these masses are not necessarily related this mass splitting can be made small enough so that co-annihilation is effective. In 5-D, the Dirac and Majorana masses of the DM state are naturally similar so that a much larger mass splitting is induced negating the efficiency of the co-annihilation process. Fortunately, unlike in 4-D, in 5-D the original Dirac fermion easily obtains parity-violating couplings to the DP KK tower states which are inherited by the physical Majorana fields. This leads to a new coupling of the DM to the DP which is diagonal as well as axial-vector in nature thus leading to a DM p -wave annihilation process which is needed to avoid the CMB and 21 cm constraints yet can lead to the observed relic density. Unfortunately, this coupling leads to scattering off of electrons which is velocity suppressed. DP direct production signals in this case can be more complex than in the Dirac scenario, even for just the first two DP KK states.

The extension of the 4-D KM/vector portal to 5-D opens several new windows of opportunity for model building and needs to be examined in more detail than the preliminary studies we have made here.

Acknowledgements

The author would like to particularly thank J.L. Hewett for very valuable discussions. This work was supported by the Department of Energy, Contract DE-AC02-76SF00515.

References

- [1] For a recent review of WIMPs, see G. Arcadi, M. Dutra, P. Ghosh, M. Lindner, Y. Mambrini, M. Pierre, S. Profumo and F. S. Queiroz, arXiv:1703.07364 [hep-ph].
- [2] M. Kawasaki and K. Nakayama, Ann. Rev. Nucl. Part. Sci. **63**, 69 (2013) [arXiv:1301.1123 [hep-ph]].
- [3] P. W. Graham, I. G. Irastorza, S. K. Lamoreaux, A. Lindner and K. A. van Bibber, Ann. Rev. Nucl. Part. Sci. **65**, 485 (2015) [arXiv:1602.00039 [hep-ex]].
- [4] J. Alexander *et al.*, arXiv:1608.08632 [hep-ph].
- [5] M. Battaglieri *et al.*, arXiv:1707.04591 [hep-ph].
- [6] There has been a huge amount of work on this subject; see, for example, D. Feldman, B. Kors and P. Nath, Phys. Rev. D **75**, 023503 (2007) [hep-ph/0610133]; D. Feldman, Z. Liu and P. Nath, Phys. Rev. D **75**, 115001 (2007) [hep-ph/0702123 [HEP-PH]]; M. Pospelov, A. Ritz and M. B. Voloshin, Phys. Lett. B **662**, 53 (2008) [arXiv:0711.4866 [hep-ph]]; M. Pospelov, Phys. Rev. D **80**, 095002 (2009) [arXiv:0811.1030 [hep-ph]]; H. Davoudiasl, H. S. Lee and W. J. Marciano, Phys. Rev. Lett. **109**, 031802 (2012) [arXiv:1205.2709 [hep-ph]] and Phys. Rev. D **85**, 115019 (2012) doi:10.1103/PhysRevD.85.115019 [arXiv:1203.2947 [hep-ph]]; R. Essig *et al.*, arXiv:1311.0029 [hep-ph]; E. Izaguirre, G. Krnjaic, P. Schuster and N. Toro, Phys. Rev. Lett. **115**, no. 25, 251301 (2015) [arXiv:1505.00011 [hep-ph]]; For a general overview and introduction to this framework, see D. Curtin, R. Essig, S. Gori and J. Shelton, JHEP **1502**, 157 (2015) [arXiv:1412.0018 [hep-ph]].

- [7] B. Holdom, Phys. Lett. **166B**, 196 (1986) and Phys. Lett. B **178**, 65 (1986); K. R. Dienes, C. F. Kolda and J. March-Russell, Nucl. Phys. B **492**, 104 (1997) [hep-ph/9610479]; F. Del Aguila, Acta Phys. Polon. B **25**, 1317 (1994) [hep-ph/9404323]; K. S. Babu, C. F. Kolda and J. March-Russell, Phys. Rev. D **54**, 4635 (1996) [hep-ph/9603212]; T. G. Rizzo, Phys. Rev. D **59**, 015020 (1998) [hep-ph/9806397].
- [8] See, for example, I. Antoniadis, Phys. Lett. B **246**, 377 (1990); K. R. Dienes, E. Dudas and T. Gherghetta, Phys. Lett. B **436**, 55 (1998) [hep-ph/9803466] and Phys. Lett. B **436**, 55 (1998) [hep-ph/9803466]; I. Antoniadis, N. Arkani-Hamed, S. Dimopoulos and G. R. Dvali, Phys. Lett. B **436**, 257 (1998) [hep-ph/9804398]; N. Arkani-Hamed, S. Dimopoulos and G. R. Dvali, Phys. Lett. B **429**, 263 (1998) [hep-ph/9803315]; L. Randall and R. Sundrum, Phys. Rev. Lett. **83**, 3370 (1999) [hep-ph/9905221]; T. Appelquist, H. C. Cheng and B. A. Dobrescu, Phys. Rev. D **64**, 035002 (2001) [hep-ph/0012100].
- [9] T. G. Rizzo, arXiv:1801.08525 [hep-ph].
- [10] For earlier related work employing a modified warped RS setup, see K. L. McDonald and D. E. Morrissey, JHEP **1005**, 056 (2010) [arXiv:1002.3361 [hep-ph]] and JHEP **1102**, 087 (2011) [arXiv:1010.5999 [hep-ph]].
- [11] See, for example, K. R. Dienes and B. Thomas, Phys. Rev. D **85**, 083523 (2012) [arXiv:1106.4546 [hep-ph]] and Phys. Rev. D **85**, 083524 (2012) [arXiv:1107.0721 [hep-ph]] and subsequent works.
- [12] P. A. R. Ade *et al.* [Planck Collaboration], Astron. Astrophys. **594**, A13 (2016) [arXiv:1502.01589 [astro-ph.CO]].
- [13] H. Liu, T. R. Slatyer and J. Zavala, Phys. Rev. D **94**, no. 6, 063507 (2016) [arXiv:1604.02457 [astro-ph.CO]]. See also, M. Dutra, M. Lindner, S. Profumo, F. S. Queiroz, W. Rodejohann and C. Siqueira, arXiv:1801.05447 [hep-ph].
- [14] J. D. Bowman, A. E. E. Rogers, R. A. Monsalve, T. J. Mozdzen and N. Mahesh, Nature **555**, no. 7694, 67 (2018). doi:10.1038/nature25792
- [15] T. R. Slatyer and C. L. Wu, Phys. Rev. D **95**, no. 2, 023010 (2017) doi:10.1103/PhysRevD.95.023010 [arXiv:1610.06933 [astro-ph.CO]].
- [16] See, for example, H. Liu and T. R. Slatyer, arXiv:1803.09739 [astro-ph.CO]; S. Clark, B. Dutta, Y. Gao, Y. Z. Ma and L. E. Strigari, arXiv:1803.09390 [astro-ph.HE]; A. Mitridate and A. Podo, arXiv:1803.11169 [hep-ph].
- [17] G. Steigman, Phys. Rev. D **91**, no. 8, 083538 (2015) [arXiv:1502.01884 [astro-ph.CO]].
- [18] J. L. Feng and J. Smolinsky, Phys. Rev. D **96**, no. 9, 095022 (2017) [arXiv:1707.03835 [hep-ph]]. See also, B. Li and Y. F. Zhou, Commun. Theor. Phys. **64**, no. 1, 119 (2015) [arXiv:1503.08281 [hep-ph]] and B. Li and Y. F. Zhou, Commun. Theor. Phys. **64**, no. 1, 119 (2015) [arXiv:1503.08281 [hep-ph]].
- [19] G. R. Dvali, G. Gabadadze and M. A. Shifman, Phys. Lett. B **497**, 271 (2001) [hep-th/0010071]; M. Carena, E. Ponton, T. M. P. Tait and C. E. M. Wagner, Phys. Rev. D **67**, 096006 (2003) [hep-ph/0212307]; M. Carena, T. M. P. Tait and C. E. M. Wagner, Acta Phys. Polon. B **33**, 2355 (2002) [hep-ph/0207056]; F. del Aguila, M. Perez-Victoria and J. Santiago, Acta Phys. Polon. B **34**, 5511 (2003) [hep-ph/0310353] and JHEP **0302**, 051 (2003) [hep-th/0302023]; H. Davoudiasl, J. L. Hewett and T. G. Rizzo, Phys. Rev. D **68**, 045002 (2003) [hep-ph/0212279] and JHEP **0308**, 034 (2003) [hep-ph/0305086].
- [20] See, for example, A. Muck, A. Pilaftsis and R. Ruckl, Phys. Rev. D **65**, 085037 (2002) [hep-ph/0110391]; T. Flacke, A. Menon and D. J. Phalen, Phys. Rev. D **79**, 056009 (2009) [arXiv:0811.1598 [hep-ph]].
- [21] For a recent update, see D. Sperka (ATLAS Collaboration) and A.C. Marini (CMS Collaboration), talks given at the *5^{3^d}* Rencontres de Moriond Electroweak Interactions and Unified Theories, La Thuile, Italy, 10-17 March 2018.

- [22] T.T. Yu (SENSEI Collaboration), talk given at the 2018 UCLA Dark Matter meeting, UCLA, 21-23 Feb. 2018.
- [23] R. Essig, T. Volansky and T. T. Yu, Phys. Rev. D **96**, no. 4, 043017 (2017) [arXiv:1703.00910 [hep-ph]].
- [24] R. Essig, M. Fernandez-Serra, J. Mardon, A. Soto, T. Volansky and T. T. Yu, JHEP **1605**, 046 (2016) [arXiv:1509.01598 [hep-ph]].
- [25] See, for example, A. Ahmed, M. Duch, B. Grzadkowski and M. Iglicki, arXiv:1710.01853 [hep-ph].
- [26] N. Baltzell *et al.* [HPS Collaboration], Nucl. Instrum. Meth. A **859**, 69 (2017) [arXiv:1612.07821 [physics.ins-det]].
- [27] For more information about the LDMX experiment, see <https://confluence.slac.stanford.edu/display/MME/Light+Dark+Matter+Experiment> and also T. Raubenheimer *et al.*, arXiv:1801.07867 [physics.acc-ph].
- [28] We follow the flat space limit of the work in S. J. Huber and Q. Shafi, Phys. Lett. B **583**, 293 (2004) [hep-ph/0309252].